Probing the Symmetry of the Nonlinear Optic Chromophore Ru(*trans*-4,4′-diethylaminostyryl-2,2′-bipyridine)$_3^{2+}$: Insight from Polarized Hyper-Rayleigh Scattering and Electroabsorption (Stark) Spectroscopy

Fredrick W. Vance and Joseph T. Hupp*

Contribution from the Department of Chemistry and Materials Research Center, Northwestern University, Evanston, Illinois 60208

Received November 19, 1998

Abstract: Polarized hyper-Rayleigh scattering (HRS) has been used to interrogate a putative octupolar "super" chromophore Ru(*trans*-4,4′-diethylaminostyryl-2,2′-bipyridine)$_3^{2+}$. While the hyperpolarizability (β) is impressive, it is apparent from polarized HRS measurements that the symmetry of the excited state, and thus the hyperpolarizability tensor, is best described as dipolar in nature. Electroabsorption (electronic Stark effect) experiments support these findings, implying that changes in dipole moment ($\Delta\mu$) accompany optical excitation. The measured $|\Delta\mu|$ contributions from both metal-to-ligand charge transfer and intraligand transitions have been used to model the wavelength-dependent hyperpolarizability; reasonable qualitative agreement between experimental results and a simple three-state, two-level dipolar model is obtained.

Introduction

The requirements for generation of large second-order nonlinear optical (NLO) responses from molecular materials have led researchers to develop an enormous number of organic, inorganic, and organometallic chromophores based on linear or approximately linear donor−acceptor geometries.[1,2] The best chromophores of this genre are those which simultaneously optimize oscillator strengths, *f*, and ground-state/excited-state dipole moment changes, $\Delta\mu$, while minimizing the differences in energy between charge-transfer transitions and incident (ω) and/or emitted (2ω) photons. To some extent the desired optimizations of *f* and $\Delta\mu$ pose conflicting chromophore design requirements.[3] Good compromises have been achieved, however, by placing extended conjugated bridges between electron acceptor and donor moieties. Indeed, based on this strategy, several chromophores exhibiting large molecular first hyperpolarizabilities at potentially technologically useful wavelengths, i.e., $\beta(\omega)$ values in excess of 2000×10^{-30} esu, have now been developed.[4,5]

Despite these successes, an alternative strategy based on octupolar chromophores has recently attracted considerable attention (see Figure 1).[6,7] One reason for the attention has been the realization that for device applications octupolar chromophores offer a potentially significant structural advantage over their dipolar counterparts. Since the macroscopic susceptibility of a material depends on the orientation of the molecules in the bulk phase, the chromophores must align such that their molecular susceptibility is additive. This requirement is often not met by materials composed of dipolar molecules; the vectorial nature of the dipolar chromophore often promotes crystallization in a centrosymmetric fashion—for example, crystallization in an antiparallel dipole configuration—thereby negating the microscopic dipole. For purely octupolar chromophores, however, the tendency toward antiparallel dipolar crystallization is fully circumvented by the strict cancellation of all molecular dipole vector components. (Of course, noncentrosymmetric crystallization of the molecular octupole is still required for induction of macroscopic second-order optical susceptibility.)

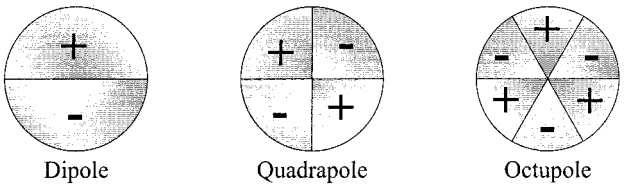

Figure 1. The number of nodes (*J*) needed to describe a charge distribution will determine whether an irreducible symmetry group has dipolar ($J = 1$), quadrupolar ($J = 2$), or octupolar ($J = 3$) character. Note that, while higher order multipoles do exist ($J > 3$), β can only have components of $J = 1$ and $J = 3$ (see ref 6). Note also that the figure shows only one of many possible representations of an octupolar charge distribution. A three-dimensional object with D_{3h} symmetry and a difference in charge density for the interior versus the exterior also possesses an octupole moment.

Ironically, the dipolar vector cancellation effect has, until recently, served to hinder the investigation of octupolar chromophores. The difficulties have arisen because the most popular and convenient experimental technique for characterizing isolated second-order molecular NLO responses, i.e., electric field induced second harmonic generation (EFISHG), requires that a candidate chromophore possess a net ground-state dipole

* E-mail: jthupp@chem.nwu.edu.

(1) Kanis, D. R.; Ratner, M. A.; Marks, T. J. *Chem. Rev.* **1994**, *94*, 195.
(2) Long, N. J. *Angew. Chem., Int. Ed. Engl.* **1995**, *34*, 21.
(3) Marder, S. R.; Beratan, D. N., Cheng, L.-T. *Science* **1991**, *252*, 103.
(4) Marder, S. R.; Cheng, L.-T.; Tiemann, B. G.; Friedli, A. C.; Blanchard-Desce, M.; Perry, J. W.; Skinhøj, J. *Science* **1994**, *263*, 511.
(5) LeCours, S. M.; Guan, H.-W.; DiMagno, S. G.; Wang, C. H., Therien, M. J. *J. Am. Chem. Soc.* **1996**, *118*, 1497.
(6) Zyss, J.; Ledoux, I. *Chem. Rev.* **1994**, *94*, 77.
(7) Zyss, J.; Dhenaut, C.; Chauvan, T.; Ledoux, I. *Chem. Phys. Lett.* **1993**, *206*, 409.

10.1021/ja9840044 CCC: $18.00
Published on Web 04/28/1999

moment. To prevent migration, the EFISHG methodology also requires that candidate chromophores be neutral. The recent emergence of an alternative methodology, hyper-Rayleigh scattering (HRS) spectroscopy, has broadened this area of research by allowing for solution-phase investigation of candidate NLO chromophores which lack permanent dipole moments[8−12] or possess a net molecular charge.[13−16]

In this work we have investigated the symmetry of selected optical transitions in a dipositive transition-metal complex (**1**) comprised of Ru^{II} and three bidentate ligands (**2**). This complex

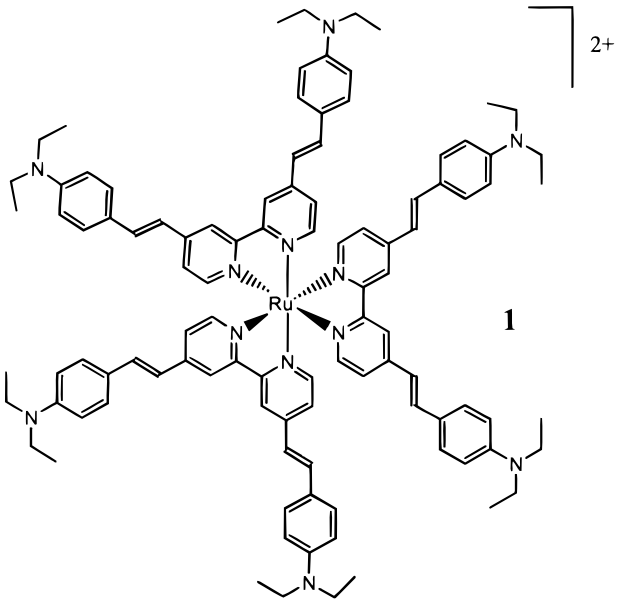

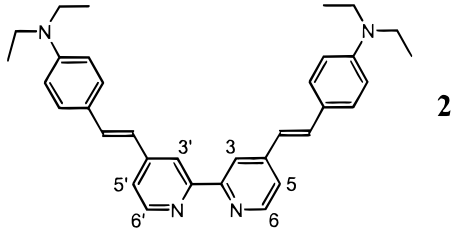

is nearly identical to one previously shown to exhibit an exceptionally large molecular hyperpolarizability.[17,18] In the earlier report, the large hyperpolarizability was ascribed to an unusually effective octupolar scattering mechanism. Indeed, if the octupolar description is valid, the ruthenium complex would clearly be the single most efficient octupolar scatterer described to date. Our investigations via resonant HRS and electroabsorption (Stark) spectroscopy were designed to probe whether the octupolar symmetry is maintained in the relevant molecular excited states or whether lower symmetry dipolar excited states are created such that second-order NLO responses arise from a more conventional mechanism. As discussed below, this interesting question is equivalent, for metal-to-ligand charge transfer (MLCT) excited states, to the often-asked question of whether such states feature symmetrically delocalized electronic charges or whether the charges are instantaneously localized on a single ligand (eq 1).[19−22]

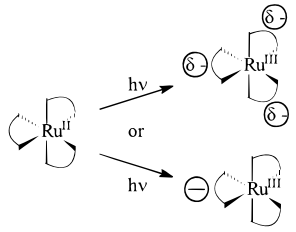

(1)

Background. Theoretical aspects of hyper-Rayleigh scattering (HRS) have been described in detail elsewhere[23] and as such will be discussed only briefly here. Basically, the technique entails focusing a radiation source of intensity $I(\omega)$ on an isotropic sample. The resulting incoherently scattered light which is doubled in frequency, $I(2\omega)$, is HRS. This arises on a molecular scale from the molecular first hyperpolarizability, β_{ijk}, which corresponds to the second term in the expansion of the dipole moment induced by an electric field. (Here i, j, and k are the molecular coordinate indices (numbers).) The light induces a moment in each molecule that is proportional to β. For an isotropic ensemble of these molecules, the *average* induced moment will be zero, but the *variance* in the induced moment due to orientational fluctuations will be proportional to the number of molecules in a given volume element.[23,24] It is this variance which gives rise to net hyper-Rayleigh scattering, $I(2\omega)$, making it an experimentally observable, albeit small, quantity.

If the incident light of frequency ω travels in the x-direction and is polarized in the z-direction, and if the detector is placed in the y-direction, then the intensity of the light hitting the detector polarized in the z-direction with a frequency of 2ω will be described by[23]

$$I_z(2\omega) = GI_z^2(\omega)\sum_n N_n\langle\beta_{zzz}^2\rangle_n \qquad (2)$$

Here, the summation over n is for the different components in the sample, N is the number density of each component (cm^{-3}), G is a parameter that accounts for collection efficiencies and local field corrections, and the brackets indicate orientational averaging. In the cases presented here, only two-component systems will be discussed (solvent and chromophore). If a component is additionally able to absorb either the incident or

(8) Clays, K.; Persoons, A. *Rev. Sci. Instrum.* **1994**, *65*, 2190.
(9) Verbeist, T.; Clays, K.; Samyn, C.; Wolff, J.; Reinhoudt, D.; Persoons, A. *J. Am. Chem. Soc.* **1994**, *116*, 9320.
(10) Stadler, S.; Dietrich, R.; Bourhill, G.; Bräuchle, Ch. *Opt. Lett.* **1996**, *21*, 251.
(11) Kaatz, P.; Shelton, D. P. *J. Chem. Phys.* **1996**, *105*, 3918.
(12) Hendrickx, E.; Vinckier, A.; Clays, K.; Persoons, A. *J. Phys. Chem.* **1996**, *100*, 19672.
(13) Coe, B. J.; Chamberlain, M. C.; Essex-Lopresti, J. P.; Gaines, S.; Jeffery, J. C.; Houbrechts, S.; Persoons, A. *Inorg. Chem.* **1997**, *36*, 3284.
(14) Hendrickx, E.; Clays, K.; Persoons, A.; Dehu, C.; Brédas, J. L. *J. Am. Chem. Soc.* **1995**, *117*, 3547.
(15) Clays, K.; Hendrickx, E.; Triest, M.; Persoons, A. *J. Mol. Liq.* **1995**, *67*, 133.
(16) Morrison, I. D.; Denning, R. G.; Laidlaw, W. M.; Stammers, M. A. *Rev. Sci. Instrum.* **1996**, *67*, 1445.
(17) Dhenaut, C.; Ledoux, I.; Samuel, I. D. W.; Zyss, J.; Bourgault, M.; Le Bozec, H. *Nature* **1995**, *374*, 339.
(18) The magnitude of β measured at 1320 nm (incident light wavelength) was reported[17] to be 2200×10^{-30} esu.
(19) Li, C.; Hoffman, M. Z. *Inorg. Chem.* **1998**, *37*, 830.
(20) Dallinger, R. F.; Woodruff, W. H. *J. Am. Chem. Soc.* **1979**, *101*, 4391.
(21) Oh, D. H.; Boxer, S. G. *J. Am. Chem. Soc.* **1989**, *111*, 1130.
(22) Casper, J. V.; Westmoreland, T. D.; Allen, G. H.; Bradley, P. G.; Meyer, T. J.; Woodruff, W. H. *J. Am. Chem. Soc.* **1984**, *106*, 3492.
(23) Clays, K.; Persoons, A.; De Maeyer, L. *Adv. Chem. Phys.* **1994**, *85*, 455.
(24) For example (from ref 23), if there is a single hyperpolarizability component, β_{333}, and the light is z-polarized, the variance induced in the x direction due to orientational fluctuations is described as follows (where N is the number of chromophores and v is the volume):

$$\langle B_x^2\rangle = \frac{1}{35}\frac{N\beta_{333}^2}{v^2}$$

doubled radiation, then an absorption correction must be applied. For example, for a two-component system where the chromophore absorbs light at the doubled frequency (2ω) but the solvent does not, eq 2 can be rewritten as

$$\frac{I_z(2\omega)}{I_z^2(\omega)} = G(N_s\langle\beta_{zzz}{}^2\rangle_s + N_c\langle\beta_{zzz}{}^2\rangle_c)e^{-N_c\sigma_c(2\omega)l_c} \qquad (3)$$

where subscripts s and c denote solvent and chromophore, $\sigma(2\omega)$ is the molecular cross section at the harmonic frequency (cm^2), and l is the effective optical path length (cm). The exponential term in eq 3 accounts for losses due to absorption and can thus be omitted when the system is transparent. In the internal reference method, the HRS signal is measured as a function of chromophore concentration and the solvent acts as an internal standard.[25] A plot of $I(2\omega)/I^2(\omega)$ versus concentration of chromophore will yield an intercept due to hyper-Rayleigh scattering by the solvent, a slope proportional to the square of the hyperpolarizability of the chromophore, and an exponential decay coefficient encompassing the absorption cross section and optical path length.[26]

The amount of polarization that is maintained in the signal is useful in assessing the individual components of the total hyperpolarizability tensor. To establish the relationship of the laboratory frame to the molecular frame, it is important to note that eqs 2 and 3 can easily be adapted for detection of *x*-polarized light (again with *z*-polarized incident light):

$$\frac{I_x(2\omega)}{I_z^2(\omega)} = G(N_s\langle\beta_{xzz}{}^2\rangle_s + N_c\langle\beta_{xzz}{}^2\rangle_c)e^{-N_c\sigma_c(2\omega)l_c} \qquad (4)$$

Notice that the only changes from eq 3 are the indices of the detected polarization and the hyperpolarizability tensor. Because the sample is isotropic, using other linear polarization schemes (e.g., I_y) yields no further information about the hyperpolarizability tensor. It should be noted, however, that elliptically polarized light can be used in HRS to assess up to five independent experimental quantities.[11] Nevertheless, only linearly polarized light has been used for this work.

Experimental Section

Synthesis. The ligand *trans*-4,4′-diethylaminostyryl-2,2′-bipyridine (DEAS, **2**) was prepared according to literature techniques.[27] The complex $[Ru(DEAS)_3](PF_6)_2{\cdot}2H_2O$ (**1**) was prepared by adding 90 mg (18×10^{-5} mol) of **2** to 16 mg (6×10^{-5} mol) of $RuCl_3{\cdot}3H_2O$ (Alfa Aesar) in 10 mL of dimethyl formamide (Fisher).[17] The mixture was heated to reflux for 4 h, producing a brick red solution. An aqueous solution of tetrabutylammonium hexafluorophosphate (Aldrich; 50 mL, 48×10^{-4} M) was used to precipitate the product, which was then dissolved in acetone and purified via chromotography on an alumina column with 3:1 acetone:methanol as the eluant. Finally, the isolated product was recrystallized from 1:2 acetone:water. ^{1}H NMR spectrum in d_6-acetone solution: δ 8.96 (s, 3,3′), 7.91 (d, 6,6′, $J = 6$ Hz), 7.71 (d, CH═CH, $J = 16$ Hz), 7.61 (d, 5,5′, $J = 6$ Hz), 7.52 (d, ArH, $J = 9$ Hz), 7.09 (d, CH═CH, $J = 16$ Hz), 6.76 (d, ArH, $J = 9$ Hz), 3.47 (q, CH_2CH_3, $J = 7$ Hz), 2.96 (s, H_2O), 1.18 (t, CH_2CH_3, $J = 7$ Hz). Elem. anal. found (calcd): C, 63.39% (63.31%); H, 5.84% (6.15%); N, 8.84% (8.69%). Electrospray mass spectrometry in MeOH (performed on a Micromass Quattro II) showed the expected peak for the 2+ cation at $m/z = 804.5$ (804.4 calcd) as well as the 3+ cation at $m/z = 536.8$ (536.3 calcd). Furthermore, the spectra exhibited the expected isotopic distributions. No evidence was found for higher mass species such as the 1+ cation.

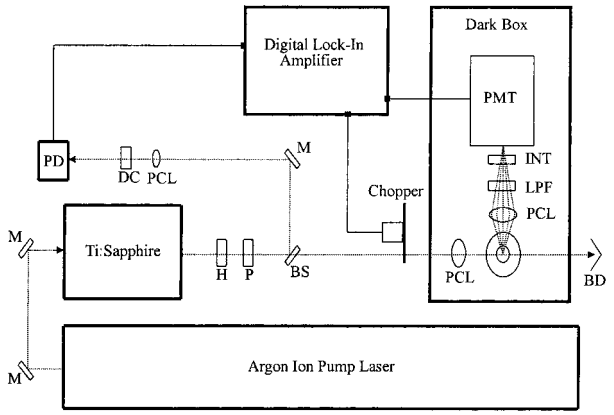

Figure 2. Schematic representation of laser and collection apparatus used in hyper-Rayleigh scattering experiment. BD = beam dump, BS = beam splitter, H = half-wave plate, INT = interference filter, LPF = low-pass filter, M = mirror, P = femtosecond polarizer, PCL = planoconvex lens, PD = photodiode, PMT = photomultiplier tube.

Hyper-Rayleigh Scattering. The intensity of scattered light at the doubled frequency relevant to the incident radiation was obtained by using a mode-locked Ti:sapphire laser system.[8] A schematic representation can be found in Figure 2. The Ti:Sapph laser (Spectra-Physics, Model 360 "Tsunami") typically produces 1 W of average power in a train of pulses nominally 100 fs in duration at a repetition rate of 82 MHz. The intensity of the light is modulated by rotation of a half-wave plate placed before a linear polarizer. (Since HRS is not a time-dependent phenomenon, the pulse duration itself is not an important parameter. However, since both the polarization and instantaneous power are important, care was taken to use suitable optics throughout the experiment to minimize pulse distortions.)[8] The light source is chopped at a rate of approximately 1 kHz before being focused onto the sample. A small portion of the beam (~10%) is passed through a doubling crystal before striking a photodiode. In this manner, the incident radiation can be monitored not only for its average power, but also for the relative stability of mode-locking.

The scattered light was collected using two convex lenses and passed through a low-pass filter and a notch filter centered at 410 nm before being detected via a photomultiplier tube (PMT). The signal was retrieved with a digital lock-in amplifier and was recorded via computer along with the reference signal from the photodiode. For polarization studies, a dichroic sheet polarizer was rotated in front of the PMT, and collection optics were replaced with an iris to reduce the numerical aperture.

Electroabsorption (Stark) Spectroscopy. The electroabsorption measurements were conducted at 77 K in a manner described previously.[28,29,30] The solvent (glass) used was a 1:1 (v:v) mixture of butyronitrile and 2-methyltetrahydrofuran. The low-temperature absorption spectrum was fit to a combination of Gaussian peaks using PeakFit software (SPSS Inc., Chicago, IL). These peaks (and their derivatives) were then used to model the electroabsorption spectra (again using PeakFit) as described below. The process was iterated until satisfactory fits to both the absorption and electroabsorption spectra were obtained.

Results

Linear Absorption. Figure 3 shows absorption spectra for compounds **1** and **2**. The intense transition centered at ~410 nm ($\epsilon_{max} = 33\,200\ M^{-1}\ cm^{-1}$) for **2** roughly triples in intensity upon formation of complex **1** ($\epsilon_{max} = 116\,000\ M^{-1}\ cm^{-1}$)—con-

(25) N_s is essentially constant in the low solute concentration range studied.

(26) This method proved reliable in providing consistent, reproducible results. The quantitative validity of the method as compared to an external standard method has been discussed at length. See, for example: (a) Pauley, M. A.; Guan, H.-W.; Wang, C. H.; Jen, A. K.-Y. *J. Chem. Phys.* **1996**, *104*, 7821. (b) ref 16.

(27) Juris, A.; Campagna, S.; Bidd, I.; Lehn, J.-M.; Ziessel, R. *Inorg. Chem.* **1988**, *27*, 4007.

(28) Karki, L.; Lu, H. P.; Hupp, J. T. *J. Phys. Chem.* **1996**, *100*, 15637.

(29) Karki, L.; Hupp, J. T. *J. Am. Chem. Soc.* **1997**, *119*, 4070.

(30) Karki, L.; Hupp, J. T. *Inorg. Chem.* **1997**, *36*, 3318.

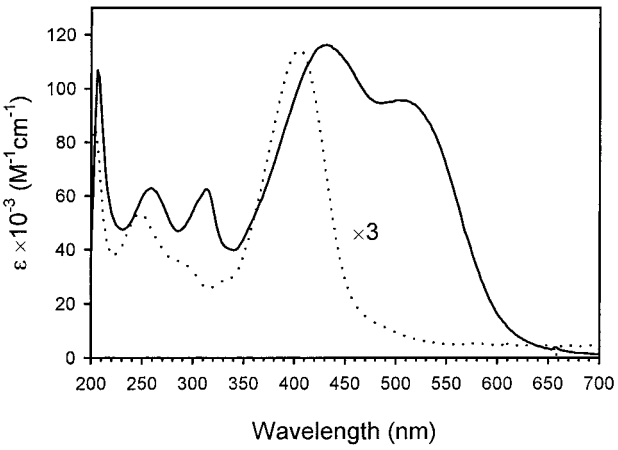

Figure 3. Absorption spectra of **1** (solid line) and **2** (dotted line, shown at 3× magnification).

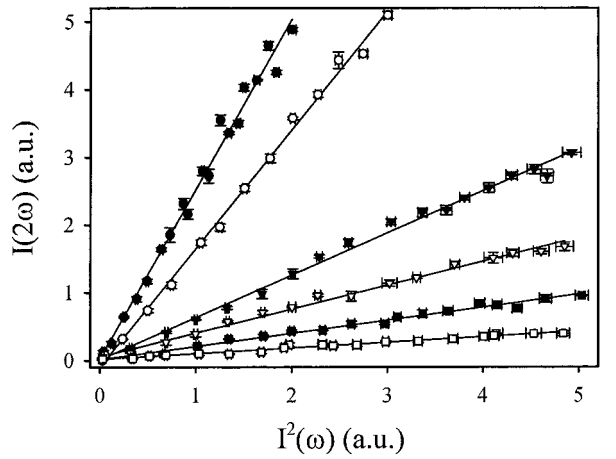

Figure 4. Power dependence of HRS signal for **1** at various number densities: ● = 6.0×10^{15} cm^{-3} (10 μM), ○ = 3.6×10^{15} cm^{-3} (6.0 μM), ▼ = 1.2×10^{15} cm^{-3} (2.0 μM), ▽ = 6.0×10^{14} cm^{-3} (1.0 μM), ■ = 2.4×10^{14} cm^{-3} (0.40 μM), □ = pure water.

sistent with the presence of three ligands in one compound. Accompanying this increase is a slight red shift to ~430 nm, possibly due to overlap with the metal-to-ligand charge transfer (MLCT) band found at ~510 nm. A more probable explanation is that the intraligand absorption is charge-transfer-based and is shifted to lower energy because metal cation binding renders the pyridyl nitrogen a better electron acceptor.[31]

Hyper-Rayleigh Scattering. The HRS measurements on compounds **1** and **2** produced results consistent with signals arising entirely from their molecular hyperpolarizability. Figure 4 shows the dependence on power for compound **1**, where the expected quadratic power dependence is displayed for the entire concentration range studied. Ruled out, in part on the basis of polarization studies (below), was an alternative interpretation involving two-photon induced luminescence. This phenomenon is known to interfere with the observation of HRS from the parent 2,2′-bipyridyl complex.[16] The absence of luminescence interference in the HRS spectroscopy of **1** is consistent with the complete (within experimental error) suppression of *one*-photon luminescence—which, in turn, can be attributed to the proximity of six highly efficient excited-state redox quenchers

(31) The assignment of the 430 nm band as an IL transition is supported by an acid addition experiment. Protonating the ammine nitrogens causes the band to shift to ca. 320 nm while leaving the 510 nm band relatively unperturbed. If the 430 nm band had been MLCT in nature, protonation would have created a better electron acceptor and caused the band to red shift.

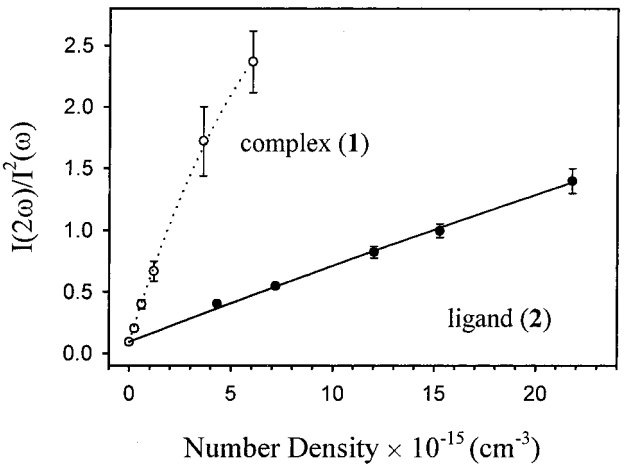

Figure 5. Concentration dependence of HRS signal for **1** (○) and **2** (●) with fits to eq 3.

(ligand amine substituents) and six probable energy-transfer quenchers (ligand styryl functionalities).

Figure 5 shows the concentration dependence of $I(2\omega)$ for both compounds. The curvature in the plots implies intensity attenuation due to absorption corresponding to an effective path length of ca. 0.5 cm, which is indeed half the width of the cells used. More significant are the relative values of the slopes and the corresponding $|\beta|$ values. By using MeOH as the internal reference (total absolute hyperpolarizability = 0.69×10^{-30} esu[32]), the absolute values of the hyperpolarizability for compounds **1** and **2** are 6500×10^{-30} and 2200×10^{-30} esu, respectively, with relative uncertainties of approximately ±15%. Notice that no explicit assumption about symmetry has yet been made (see discussion below).

Polarized HRS. The experimental outcomes of polarized HRS studies are shown in Figure 6, where the signals have been normalized (minima set to one) for comparison. To determine the polarization ratios, the results were fit to eq 5, where y is the measured signal and x is the angle of the polarizer:

$$y = a(\cos^2(x - c)) + b \tag{5}$$

The polarization ratio is then given by

$$\frac{\langle \beta_{zzz}^2 \rangle}{\langle \beta_{xzz}^2 \rangle} = \frac{a+b}{b} \tag{6}$$

If the symmetry of a molecule is known, then the relationship between the laboratory frame and molecular frame can be established in a straightforward manner. Details of this procedure have been provided elsewhere[33] but are summarized here from recent work for only two cases of special interest.[9,11]

Case 1: Dipolar Symmetry. Here we shall consider only the most simple case of dipolar symmetry, the C_{2v} point group. If we assume that Kleinman symmetry is valid[34] and additionally assume that the chromophore of interest is planar, then the two remaining independent nonzero components of β are β_{333} and $\beta_{322} = \beta_{223}$.[35] The resulting lab to molecular frame relations

(32) Clays, K.; Persoons, A. *Phys. Rev. Lett.* **1991**, *23*, 2980.

(33) Bersohn, R.; Pao, Y.-H.; Frisch, H. L. *J. Chem. Phys.* **1966**, *45*, 3184.

(34) Kleinman, D. A. *Phys. Rev.* **1962**, *126*, 1977.

(35) The indices on the hyperpolarizability tensor are used to denote coordinates. Numbers are used to describe the relevant tensor components within the molecular framework, and letters are used to describe the components observed within the laboratory frame of reference. A more complete discussion can be found in ref 33.

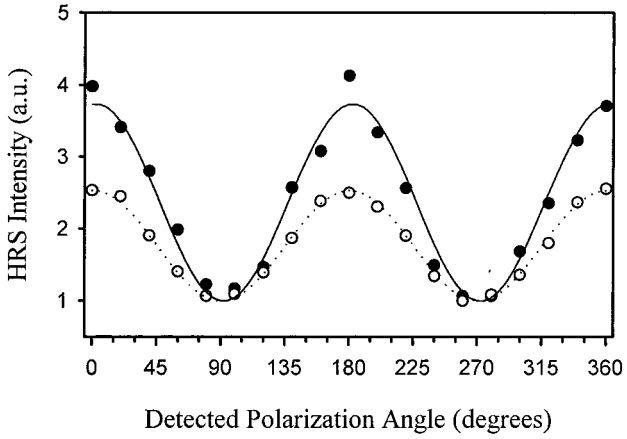

Figure 6. Polarization-dependent HRS for **1** (○) and **2** (●) with fits to eq 5. For comparison, the minima in the signals were normalized to a value of one.

are given in eqs 7 and 8:[11]

$$\langle\beta_{zzz}{}^2\rangle = \frac{1}{105}\beta_{333}{}^2\left[15 + 18\left(\frac{\beta_{322}}{\beta_{333}}\right) + 27\left(\frac{\beta_{322}}{\beta_{333}}\right)^2\right] \quad (7)$$

$$\langle\beta_{xzz}{}^2\rangle = \frac{1}{105}\beta_{333}{}^2\left[3 + 2\left(\frac{\beta_{322}}{\beta_{333}}\right) + 11\left(\frac{\beta_{322}}{\beta_{333}}\right)^2\right] \quad (8)$$

If $R = \beta_{322}/\beta_{333}$, then the polarization ratio is given by

$$\frac{I_z(2\omega)}{I_x(2\omega)} = \frac{\langle\beta_{zzz}{}^2\rangle}{\langle\beta_{xzz}{}^2\rangle} = \frac{15 + 18R + 27R^2}{3 - 2R + 11R^2} \quad (9)$$

It can easily be seen that for the case where one component dominates ($\beta_{322} = 0$), the ratio reduces to a value of 5. For compound **2**, the ratio $\langle\beta_{zzz}{}^2\rangle/\langle\beta_{xzz}{}^2\rangle$ was found to be 3.8 (± 0.1). A fit to eq 9, assuming C_{2v} symmetry, yields either $R = -0.13$ or 1.86. This indicates a substantial contribution from β_{322}, as has been previously observed for chromophores of similar symmetries.[11,36]

Case 2: Octupolar Symmetry. Molecules of D_{3h} and D_3 symmetry are among those potentially capable of behaving as octupolar chromophores. In the case when Kleinman symmetry is valid, which we assume here for simplicity, their transformation from laboratory to molecular frame is identical. In both cases, there are only four nonzero β components: $\beta_{333} = -\beta_{311} = -\beta_{131} = -\beta_{113}$. These relate to the lab frame by:[9,11]

$$\langle\beta_{zzz}{}^2\rangle = \frac{24}{105}\beta_{333}{}^2 \quad (10)$$

$$\langle\beta_{xzz}{}^2\rangle = \frac{16}{105}\beta_{333}{}^2 \quad (11)$$

The resulting polarization ratio is given in eq 12:

$$\frac{I_z(2\omega)}{I_x(2\omega)} = \frac{\langle\beta_{zzz}{}^2\rangle}{\langle\beta_{xzz}{}^2\rangle} = \frac{3}{2} \quad (12)$$

For the complex **1**, the ratio $\langle\beta_{zzz}{}^2\rangle/\langle\beta_{xzz}{}^2\rangle$ was found to be 2.4 (± 0.1). This clearly is inconsistent with an octupolar scattering mechanism, since the maximum value for the ratio with this mechanism is only 1.5.[37] If the excited charge is localized on one ligand (cf. eq 1), the effective symmetry of the active chromophore may be better approximated as C_{2v}, i.e., including only one ligand and the ruthenium center. Fitting the observed polarization ratio to eq 9 produces possible values for R of −0.345 or infinity (limiting case ratio of 2.455).

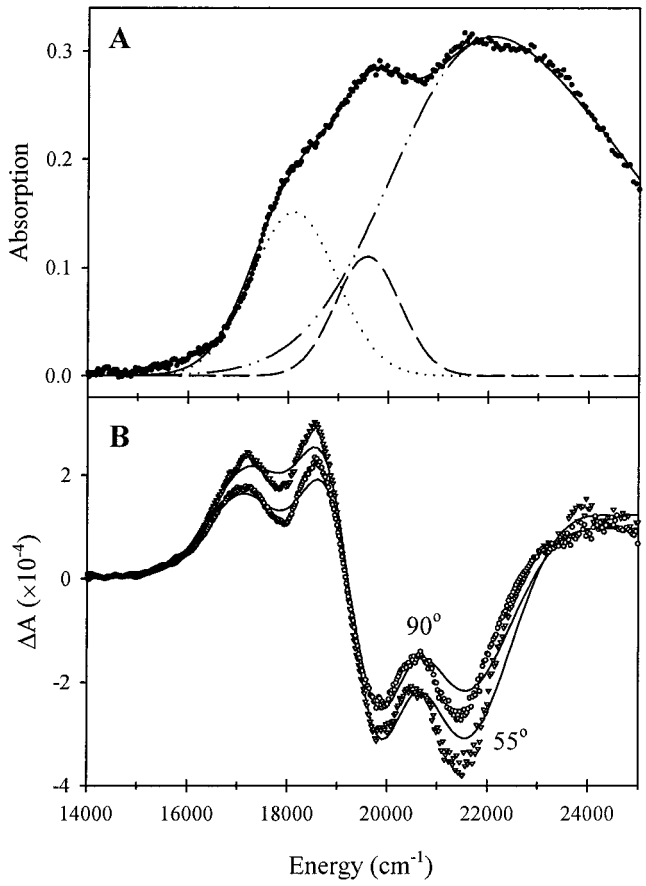

Figure 7. Electronic spectra of compound **1**. (A) Absorption of **1** at 77 K. Lines indicate component bands subsequently used to fit electroabsorption data. (B) Electroabsorption (Stark) spectra of **1** at $\chi = 55°$ (▽) and $\chi = 90°$ (○). Solid lines indicate fits to eq 13.

Electroabsorption (Stark) Spectroscopy. Figure 7 illustrates linear absorption and electroabsorption responses at 77 K for compound **1**. These were interpreted by following Liptay's analysis[38] whereby the electroabsorption signal, $\Delta A(\nu)$, is fit to a linear combination of zeroth, first, and second derivatives of the absorption band, $A(\nu)$:

$$\Delta A(\nu) = \left\{A_\chi A(\nu) + \frac{B_\chi \nu}{15hc}\frac{\mathrm{d}[A(\nu)/\nu]}{\mathrm{d}\nu} + \frac{C_\chi \nu}{30h^2c^2}\frac{\mathrm{d}^2[A(\nu)/\nu]}{\mathrm{d}\nu^2}\right\}\mathbf{F}_{\mathrm{int}}{}^2 \quad (13)$$

Here, $\mathbf{F}_{\mathrm{int}}$ is the internal electric field,[39] ν is the frequency of the absorbed light, h is Planck's constant, and c is the speed of light. As discussed in detail elsewhere,[40,41] the resulting coef-

(36) Wolff, J. J.; Längle, D.; Hillenbrand, D.; Wortmann, R.; Matschiner, R.; Glania, C.; Krämer, P. *Adv. Mater.* **1997**, *9*, 138.

(37) If Kleinman symmetry does not hold (a distinct possibility under conditions of resonant excitation), the D_3 point group has a polarization ratio of $\langle\beta_{zzz}{}^2\rangle/\langle\beta_{xzz}{}^2\rangle = 6/(4 + 7R^2)$, where $R = \beta_{123}/\beta_{333}$. The maximum polarization ratio expected is still 1.5.

(38) Wortmann, R.; Elich, K.; Liptay, W. *Chem. Phys.* **1988**, *124*, 395−409.

(39) The internal field was assumed to be 1.3 times the externally applied field.

(40) Shin, Y. K.; Brunschwig, B. S.; Creutz, C.; Sutin, N. *J. Phys Chem.* **1996**, *100*, 8157.

(41) Bublitz, G. U.; Boxer, S. G.; *Annu. Rev. Phys. Chem.* **1997**, *48*, 213.

ficients A_χ, B_χ, and C_χ provide information, respectively, about changes in the transition moment, the molecular polarizability, and the permanent dipole moment.

The absorption spectrum of **1** is composed of multiple overlapping bands that behave independently in the electroabsorption experiment. This is apparent since a single set of derivatives of the overall absorption spectra (i.e., a three-parameter fit to eq 13) does not reproduce the Stark spectra shown in Figure 7B (see the Supporting Information). In order, ultimately, to reproduce the Stark line shape, the linear absorption spectrum was fit and deconvolved by assuming three independent transitions: (1) a low-energy MLCT component centered at ~18 100 cm^{-1}, (2) an MLCT component centered at 19 600 cm^{-1}, and (3) the intense intraligand (IL) transition comprised of two bands centered at 21 400 and 23 400 cm^{-1}.[31] Given the spectral overlap, the proposed deconvolution is somewhat arbitrary. Nonetheless, the deconvolved linear components were used in eq 11 to generate a nine-parameter fit to the available electroabsorption data. Although the approach clearly does not generate a unique solution, it does provide a very approximate means for assessing contributions of individual electronic transitions to the Stark signal.[42]

From the multiparameter fit, the electroabsorption spectrum appears to be composed of significant contributions from both the B_χ and C_χ terms in eq 13 (with negligible contributions from A_χ). Since C_χ terms appear to be the dominant contributors for most of the spectrum, absorption induced changes in dipole moment, $\Delta\mu$, are likely responsible for the largest portion of the Stark signal. The C_χ coefficient can be described by

$$C_\chi = |\Delta\mu|^2[5 + (3\cos^2\chi - 1)(3\cos^2\zeta - 1)] \quad (14)$$

where χ is the angle between the incident light and applied electric field vectors (constrained by the experiment to be between zero and 90°) and ζ is the angle between the transition moment, μ_{12}, and the change in dipole moment, $\Delta\mu$. From the fits, we obtain $|\Delta\mu(\text{MLCT})|$ and $|\Delta\mu(\text{IL})|$ estimates of 7 (±1) and 16 (±2) Debye, respectively, where the errors represent uncertainties in the particular fit used in Figure 7, *not* the additional uncertainties inherent to identifying the most appropriate initial (linear) spectral parameters.

One interesting point is that the electroabsorption spectrum of this chromophore displays only a modest dependence on the angle χ. Referring to Figure 7, the magnitude of the electroabsorption signal (at its maximum) only decreases by 20−30% when χ is changed from 55° to 90°. In contrast, if μ_{12} and $\Delta\mu$ were collinear ($\zeta = 0°$), the expected decrease in the purely C_χ component of the spectrum would be 40%. Thus the transition moment and change in dipole moment vectors appear to be offset by a finite angle ζ, estimated to be between 20° and 50° for the three transitions used in the fitting procedure. As a caveat, it should be noted that the diminished dependence on χ could alternatively be interpreted as resulting from the overlapping nature of the bands themselves and an ensuing less than perfect deconvolution. If so, then the apparently anomalously weak angular dependence would provide a further indication of the nonuniqueness of fits generated by the deconvolution process.[42]

Discussion

From the polarized HRS and electroabsorption results, it is apparent that the NLO response for compound **1** is better described as arising from three (or six) dipolar transitions that are degenerate in energy, rather than from an octupolar transition (cf. eq 1). To understand better the nature of the NLO response, it is useful to consider the individual contributions of the MLCT and IL transitions to the molecular hyperpolarizabilities. One way to accomplish this, at least in an approximate fashion, is to model, within a two-level description, the wavelength-dependent hyperpolarizability (β') due to each transition:[43,44]

Scheme 1

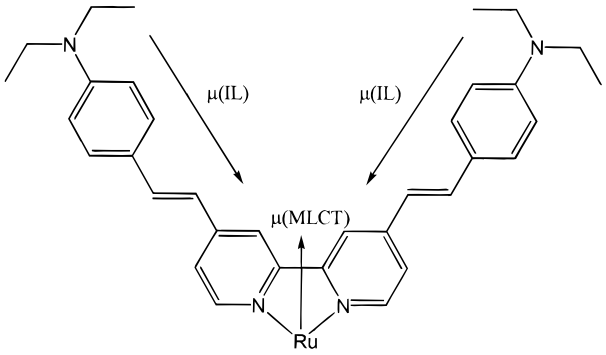

$$\beta' = \frac{3\mu_{12}^2\Delta\mu_{12}E_{op}^2}{2[E_{op}^2 - E_{inc}^2][E_{op}^2 - (2E_{inc})^2]} \quad (15)$$

Here, μ_{12} is the transition moment, $\Delta\mu_{12}$ is the change in dipole moment, E_{op} is the energy maximum of the transition, and E_{inc} is the energy of the incident radiation used. The total hyperpolarizability, β, will then be a sum of the contributions from each transition. Note that while the degeneracies of the MLCT and the IL transitions are 3 and 6, respectively, for comparison it is equally valid to consider the degeneracies to be unity since their relative contributions are accounted for in the μ_{12} term in eq 15. The transition moment is taken from the absorption spectrum according to[45]

$$\mu_{12} = (2.07 \times 10^{-2})\left(\frac{\epsilon_{max}\Delta\nu_{1/2}}{E_{op}}\right)^{1/2} \quad (16)$$

where ϵ_{max} is the molar extinction coefficient ($cm^{-1}\,M^{-1}$), $\Delta\nu_{1/2}$ is the absorption bandwidth (full width at half-maximum) (cm^{-1}), and E_{op} is the absorption maximum (cm^{-1}).

While the sign of $\Delta\mu_{12}$ is not measured in the electroabsorption experiment, the sign *is* crucial in modeling the NLO response properly. If, as suggested by previous evidence, the transition involves only one ligand, then MLCT excitation yields an increase in dipole moment (since the ground-state dipole moment is necessarily zero), and thus $\Delta\mu_{12}(\text{MLCT})$ is labeled as positive. The direction of the IL transition, however, is most likely reversed (see Scheme 1) but not strictly antiparallel to the MLCT transition. Thus, the IL transition is characterized as a charge transfer in which the nominal electron donor is the alkylamine at the terminus of the ligand and the acceptor is the pyridine nitrogen attached to the metal. Note further that two

(42) For a cautionary discussion of deconvolution and "uniqueness of fit" problems in electroabsorption spectroscopy, see: Bublitz, G. U.; Laidlaw, W. M.; Denning, R. G.; Boxer, S. G. *J. Am. Chem. Soc.* **1998**, *120*, 6068. In principle, the "uniqueness" problem can be at least partially resolved by utilizing higher order Stark spectroscopy. Unfortunately, we were unable to obtain higher order signals.

(43) Oudar, J. L.; Chemla, D. S. *J. Chem Phys.* **1977**, *66*, 2664.

(44) Alternate two-level descriptions are also available, which would increase the values of β calculated here by as much as a constant factor of 4. A full discourse on conventions for NLO can be found in the following: Willetts, A.; Rice, J. E.; Burland, D. M.; Shelton, D. P. *J. Chem. Phys.* **1992**, *97*, 7590.

(45) Creutz, C.; Newton, M. D.; Sutin, N. *J. Photochem. Photobiol. A* **1994**, *82*, 47.

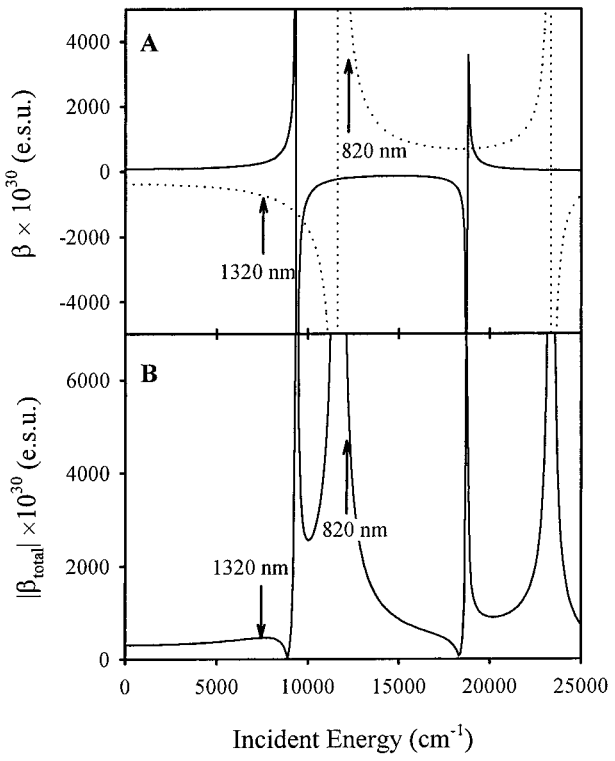

Figure 8. Energy-dependent hyperpolarizability (from eq 13): (A) Solid line = MLCT contribution (β'_{MLCT}), dotted line = IL contribution (β'_{IL}). (B) Absolute value of the total hyperpolarizability ($|\beta_{total}| = |\beta'_{MLCT} + \beta'_{IL}|$). For simplicity, the MLCT and IL transitions are regarded as perfectly antiparallel.

Table 1. Optically Derived Parameters and Calculated Hyperpolarizabilities

transition	E_{op}[a] (cm^{-1})	$\Delta\mu_{12}$[b] (e Å)	μ_{12}[a] (e Å)	$\beta_0 \times 10^{30}$ [c] (esu)	β(1320 nm) $\times 10^{30}$ (esu)	β(820 nm) $\times 10^{30}$ (esu)
MLCT	18 730	1.4	2.20	80	280	−200
IL	23 360	−3.3	3.86	−380	−750	5800
total				−300	−470	5600

[a] From room-temperature absorption measurements and eq 16. [b] From electroabsorption measurements. [c] β_0 is the calculated value at zero energy (infinite wavelength).

such transitions should exist *per* ligand, since two donor groups and two acceptor atoms are available per ligand. Since the resulting dipole will be in the opposite direction of the one formed via the MLCT transition, the sign of $\Delta\mu_{12}$(IL) is negative.[46,47] As shown in Figure 8, the summation of contributions to β (Table 1) leads to destructive interference in the low-energy regime, i.e., near the zero frequency limit. From this analysis, it is apparent that one possible improvement on the design of compound **1** would be to reverse the direction of either, but not both, of the charge-transfer transitions in the chromophore. On the other hand, over the region of energies corresponding to $E_{op}^{MLCT} < 2E_{inc} < E_{op}^{IL}$, β'_{MLCT} and β'_{IL} should be similarly signed and should *constructively* interfere.

While the calculation yields values that are in good qualitative agreement with the large hyperpolarizabilities measured for compound **1** (Table 1), two important shortcomings are worth noting: (a) the calculated $|\beta|$ value of 470×10^{-30} esu at an incident radiation wavelength of 1320 nm underestimates the experimental value of 2200×10^{-30} esu reported by Dhenaut and co-workers[17] and (b) the calculated $|\beta|$ value of 5600×10^{-30} esu with incident radiation of 820 nm also slightly underestimates the true (experimental) value of 6500×10^{-30} esu. One possible explanation is the omission of higher lying excited states from the hyperpolarizability calculations. However, without accurate electronic descriptions of these states, it is difficult to predict precisely what their contributions would be. Alternatively, both discrepancies might well be due to the omission of phenomenological "damping" terms from eq 15, such as those associated with lifetime broadening, as well as terms associated with vibronic and solvational spectral broadening. The omission of damping/broadening considerations could have significant consequences in the 820 nm irradiation case, where the scattered radiation (410 nm) is nearly resonant with the IL transition but is probably important in the 1320 nm irradiation case as well (660 nm scattering). We note, for example, that prior variable-wavelength SHG studies on poled polymers[48] and on self-assembled films[49] have shown that enhancement can be significant at wavelengths considerably further from resonance than expected from simplified two- and three-level models. A third possibility is that linear spectral deconvolution errors (see discussion above) have resulted in electroabsorption fitting errors and yielded a falsely small $\Delta\mu_{12}$ value for one of the transitions.

Conclusions

The combination of polarized resonant hyper-Rayleigh scattering and electroabsorption spectroscopies provides valuable insight into the nature of the NLO response for the ruthenium complex, **1**. While the complex exhibits impressive first hyperpolarizabilities (β values), polarization experiments indicate that these are most likely a consequence of additive resonant or near resonant dipolar responses and not a direct result of the octupolar ground-state geometry. Indeed, depending on precisely which moiety is identified as the dominant chromophore, the coordination complex can be regarded as a collection of either three or six equivalent dipolar chromophores. Electroabsorption spectroscopy supports this idea, returning $|\Delta\mu_{12}|$ values that are apparently finite for both the MLCT and IL transitions. From the $\Delta\mu_{12}$ estimates, the wavelength-dependent NLO response of **1** can be approximately modeled via a simplified three-state, two-level treatment. While the resulting calculated values for β are in good qualitative agreement with experimental measurements, they point toward the possibility of improving on the impressive NLO response for this chromophore.

Acknowledgment. R. V. Slone is gratefully acknowledged for his assistance with chromophore synthesis. We acknowledge helpful comments by Prof. George Schatz and the reviewers. This work was supported by the MRSEC program of the National Science Foundation (DMR-9632472) at the Materials Research Center of Northwestern University.

Supporting Information Available: Figure showing the result of a fit of electroabsorption data for **1** assuming only one electronic transition (PDF). This material is available free of charge via the Internet at http://pubs.acs.org.

JA9840044

(46) Since the ground-state dipole is zero by symmetry, it is equally valid to assign $\Delta\mu_{12}$(MLCT) as negative and $\Delta\mu_{12}$(IL) as positive. Since the HRS experiment measures β^2, the expected total contribution would be the same for either assignment.

(47) It is also probable that the changes in dipole moment are not in direct opposition to each other. The transition moments for the IL and MLCT transitions are almost certainly offset by some finite angle (see Scheme 1).

(48) Yitzchaik, S.; Di Bella, S.; Lundquist, P. M.; Wong, G. K.; Marks, T. J. *J. Am. Chem. Soc.* **1997**, *119*, 2995.

(49) Lundquist, P. M.; Yitzchaik, S.; Zhang, T.; Kanis, D. R.; Ratner, M. A.; Marks, T. J.; Wong, G. K. *Appl. Phys. Lett.* **1994**, *64*, 2194.